Journal of the Serbian Chemical Society
JSCS-info@shd.org.rs • www.shd.org.rs/JSCS
J. Serb. Chem. Soc. 85 (11) 1445–1462 (2020)
JSCS–5386
UDC 547.789.5/.6–304.2+544.351.3–16.032.73:519.677
Original scientific paper

DFT study and NBO analysis of solvation/substituent effects of 3-phenylbenzo[*d*]thiazole-2(3*H*)-imine derivatives

MARZIEH MIAR[1], ABOLFAZL SHIROUDI[2]*, KHALIL POURSHAMSIAN[1]**, AHMAD REZA OLIAEY[1] and FARHAD HATAMJAFARI[1]

[1]*Chemistry Department, Tonekabon Branch, Islamic Azad University, Tonekabon, Iran and* [2]*Young Researchers and Elite Club, East Tehran Branch, Islamic Azad University, Tehran, Iran*

(Received 21 April, revised 10 August, accepted 5 September 2020)

Abstract: In this work, to determine natural bond orbital (NBO) analysis, solvation and substituent effects for electron-releasing substituents (CH_3, OH) and electron-withdrawing derivatives (Cl, NO_2, CF_3) in *para* positions on the molecular structure of the synthesized 3-phenylbenzo[*d*]thiazole-2(3*H*)-imine derivatives **1**–**6** (H (**1**), CH_3 (**2**), Cl (**3**), OH (**4**), CF3 (**5**), NO_2 (**6**)) in the selected solvents (acetone, toluene, and ethanol) and gas-phase employing polarizable continuum method (PCM) model were studied at the M06-2x/6--311++G(d,p) level of theory. The relative stability of the studied compounds was affected by the possibility of intramolecular interactions between substituents and the electron donor/acceptor centers of the thiazole ring. Furthermore, atomic charges electron density, chemical thermodynamics, energetic properties, dipole moments, and the nucleus-independent chemical shifts (NICS) of the studied compounds and their relative stability are considered. The dipole moment values and the HOMO–LUMO energy gap reveal the different charge transfer possibilities within the considered molecules. Frontier molecular orbital (FMO) analysis revealed that compound **6** has very small HOMO-LUMO energy gaps in the considered phases, and thus is kinetically less stable. The obtained HOMO-LUMO energy gap corresponds to intramolecular hyperconjugative interactions π→π*. Finally, NBO analysis is carried out to demonstrate the charge transfer between localized bonds and lone pairs.

Keywords: thiazole; theoretical computations; DFT; PCM; NBO; solvent effects; dipole moment.

INTRODUCTION

Heterocycles are the largest and one of the main organic chemistry groups, and are of immense significance, not only biologically but also industrially. The

*,** Corresponding authors. E-mail: (*)abolfazl.shiroudi@iauet.ac.ir; (**)kshams49@gmail.com
https://doi.org/10.2298/JSC200421058M

most of pharmaceutical products that imitate biologically active natural products are heterocycles. Fused heterocyclic compounds are the key valuable and structural scaffolds in a wide range of natural products, drug molecules, and functional materials.[1,2] Among them, the related research on benzothiazole analogs is an organosulfur heterocyclic compound that has become a rapidly developing and increasingly active topic. The significant role of these groups of compounds lies in the fact that they are used as building blocks in organic synthesis due to their wide variety biological activities as core nucleus in various drugs such as anticancer, antimicrobial, antitumor, antibacterial, anti-HIV, antifungal, antiviral, anti-Alzheimer, antimalarial and anti-diabetic.[3–11] Hence, we report a facile, environmentally friendly method for intramolecular cyclization under solvent-free conditions. The reaction occurs, in the presence of sodium *tert*-butoxide as a strong base, in two steps. Finally, the challenges of using organic solvents in industrial processes are addressed in terms of expense of solvent, solvent stability, and solvent safety. We believe that a holistic view of the solvent effects, the mechanistic elucidation of these effects, and careful consideration of the challenges related to the solvent use may assist researchers in the selection and design improved solvent systems for targeted benzothiazole biomass conversion processes.[12]

The density functional theory (DFT) method is accepted, as a popular post-HF approach for the computation of molecular structure, and energies of molecules, by *ab initio* community. There are several basic approaches for modeling molecular systems in solution. One of them is the implicit treatment of solvent molecules,[13] self-consistent reaction-field (SCRF) models employ this approach[14] with the polarizable continuum model (PCM) being the first proposed SCRF method. The use of the PCM model in the DFT is a good method for investigating solvent effects.[15] In our pursuit of an improved synthetic method for the preparation of organic compounds, the M06-2x functional[16] using the 6-311++G(d,p) basis set[17] was used in the studied solvents (toluene, acetone, ethanol), and the obtained data was compared with the same properties in the gas phase to determine their electronic and spectroscopic properties, and to benefit from two major types of effects: solvent effects on solubility of benzothiazole components and solvent effects on chemical thermodynamics including those affecting the products.[18] Moreover an attempt is made to supply further qualitative chemical insights using the donor–acceptor interaction energies, nucleus independent chemical shift (NICS) techniques,[19–22] and natural bond orbital (NBO) analysis.[23] The goal of this analysis is to provide quantitative answers to the following questions concerning the solvent and substituent effects on the electronic structures of the considered compounds:

a) Is there a relationship between the HOMO–LUMO gaps in the con–sidered compounds?

b) How is the resonance energy related to the donor-acceptor interactions of studied molecules?

c) How do the donor-acceptor interactions influence the occupancies of the involved bonds?

In conclusion, we explain the findings obtained with the global reactivity descriptors studies in order to provide a deeper insight into the solvent and substituent effects.

THEORY AND COMPUTATIONAL DETAILS

All quantum chemical calculations were performed using the Gaussian 09 program.[24] The molecular structures were visualized based on the output data of the DFT calculations using the GaussView program.[25] Geometry optimizations and frequency calculations were carried out at the M06-2x/6-311++G(d,p) level of theory. The nature of all the optimized structures are determined based on the harmonic vibrational frequency calculations calculated at the same theoretical level to confirm that a minimum on the potential energy surface was achieved under the imposed constraint of the indicated symmetry. The NBO populations, atomic charges, frontier molecular orbital properties, dipole moments, and the second-order perturbation stabilization energy of the donor–acceptor interactions are calculated at the same level using the NBO 5.0 program.[26] Also, the aromaticity index NICS values for all the studied compounds are estimated within the gauge-included atomic orbital (GIAO) method at the same theoretical level. Finally, the geometries of the considered compounds are re-optimized at the same level in three different solvents *i.e.*, non-polar (toluene (ε = 2.374)), polar aprotic (acetone (ε = 20.493)) and polar protic (ethanol (ε = 24.852)) in order to estimate the effect of the liquid environment.

RESULTS AND DISCUSSION

Synthesis of the 3-phenylbenzo[*d*]thiazole-2(3*H*)-imine derivatives was carried out as a result of the different interactions of synthesized *N*-acyl-*N*′-aryl thioureas with diazonium salt. Optimized structures of all compounds investigated at a detailed computational level are shown in the Supplementary material for this paper (Fig. S-1 of the Supplementary material to this paper).

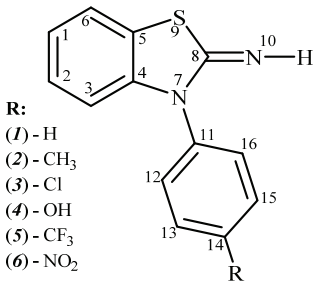

Scheme 1. The structures of the studied compounds.

Energy and thermodynamic parameters

The structures and numbering of the 3-phenylbenzo[*d*]thiazole-2(3*H*)-imine derivatives forms are represented in Scheme 1. The zero point energy (*ZPE*),

total electronic energy (E_{el}), relative energy (ΔE), corrected zero-point energy (ZPE^b), and computed corrected total energy (E_{corr}) of studied compounds (E_{corr} = = E_{el} + ZPE^b), as calculated by the density functional theory M06-2x/6-311++G(d,p) level of theory were investigated in different solvents and gas phases at T = 298 K are listed in Table I. It is noted that superscript *b* denotes the corrected by multiplying by a scaling factor (0.97).[27]

TABLE I. Total energies, relative energy (ΔE) and solvation energy (ΔE_{Solv}) of the 3-phenylbenzo[*d*]thiazole-2(3*H*)-imine derivatives (P = 1 atm, T = 298 K); ΔE_{solv} = (E_{corr}(in solvent) – E_{corr}(in gas))

Substituent	Parameter	Gas (ε = 1.0)	Toluene (ε = 2.374)	Acetone (ε = 20.493)	Ethanol (ε = 24.852)
–H (**1**)	E_{corr} / Hartree	–1008.800	–1008.819	–1008.825	–1008.822
	ΔE_{cor} / kcal* mol^{-1}	15.662	3.666	0.000	1.837
	ΔE_{Solv} / kcal mol^{-1}	0.000	–11.996	–15.662	–13.825
–CH_3 (**2**)	E_{corr} / Hartree	–1048.080	–1048.100	–1048.105	–1048.102
	ΔE_{corr} / kcal mol^{-1}	16.241	3.731	0.000	1.856
	ΔE_{Solv} / kcal mol^{-1}	0.000	–12.510	–16.241	–14.384
–Cl (**3**)	E_{corr} / Hartree	–1468.410	–1468.431	–1468.436	–1468.433
	ΔE_{corr} / kcal mol^{-1}	15.959	3.272	0.000	1.775
	ΔE_{Solv} / kcal mol^{-1}	0.000	–12.686	–15.959	–14.184
–OH (**4**)	E_{corr} / Hartree	–1084.021	–1084.042	–1084.050	–1084.049
	ΔE_{corr} / kcal mol^{-1}	18.306	5.077	0.000	0.462
	ΔE_{Solv} / kcal mol^{-1}	0.000	–13.229	–18.306	–17.844
–CF_3 (**5**)	E_{corr} / Hartree	–1345.847	–1345.866	–1345.872	–1345.869
	ΔE_{corr} / kcal mol^{-1}	15.447	3.792	0.000	1.674
	ΔE_{Solv} / kcal mol^{-1}	0.000	–11.655	–15.447	–13.774
–NO_2 (**6**)	E_{corr} / Hartree	–1213.287	–1213.308	–1213.314	–1213.310
	ΔE_{corr} / kcal mol^{-1}	17.342	3.912	0.000	2.874
	ΔE_{Solv} / kcal mol^{-1}	0.000	–13.430	–17.342	–14.468

The relative energies in acetone solvent are more stable by 0.46–18.31 kcal mol^{-1}, compared to the other ones. The major difference between obtained energies was found in the gas phase (18.31 kcal mol^{-1} for OH substituent). The order of stability in the considered solvent and gas phases is: Cl > CF_3 > NO_2 > > OH > CH_3 > H. The obtained results show that the stability increases with the increase of electron-withdrawing substituents. At the other hand, all the species were stabilized more or less by the solvent dielectric constant, where the corrected total energy (E_{corr}) decrease in polar solvents (ethanol and acetone) was more than in the non-polar solvent (toluene). The solute-solvent interactions further stabilized the structures compared to either the non-polar solvent (toluene) or in the gas phase. It is noted that the values of solvation energies (E_{solv}) are higher in the case of ethanol and acetone compared to toluene which agrees

* 1 kcal = 4184 J

with the polar character of the considered compounds (Table I). The polar solvents (ethanol and acetone) stabilized the studied compounds through hydrogen bonding and dipole-dipole interactions more than the non-polar solvent (toluene).

Dipole moments

The dipole moment (μ) prediction is an important issue which is intensely associated with the molecular stability in polar environments. In this work, the experimental dipole moment μ is not known. The calculated dipole moments in different environments (*i.e.*, toluene, acetone, ethanol) are shown in Table II. The influence of the polar environment (*i.e.*, acetone and ethanol) is notable in comparison to the dipole moment values in both phases. The order of the calculated dipole moment values is: $NO_2 > CF_3 > Cl > CH_3 > H > OH$. Among the studied compounds, molecule **6** (R=NO_2 substituent) has the highest dipole moment in the solvent and gas phases, because it has a higher dipole interaction. The order of the dipole moment determined values for molecules **1–6** in solvents with different polarity (ethanol > acetone > toluene) resulting from the increase of the dielectric constant, which corresponds to the order of the dielectric constant value to be increased with the increase of the dielectric constant (Table II).

TABLE II. Calculated dipole moment (μ / D*) of the optimized compounds **1–6** in the different phases

Compound	Medium			
	Gas (ε = 1.00)	Toluene (ε = 2.374)	Acetone (ε = 20.493)	Ethanol (ε = 24.852)
1 (R = H)	1.9064	1.9685	2.0949	2.1042
2 (R = CH_3)	2.0122	2.1487	2.2518	2.2748
3 (R = Cl)	2.6144	2.6481	2.6672	2.6940
4 (R = OH)	1.7086	2.0246	2.3897	2.4145
5 (R = CF_3)	3.7871	3.8093	3.8620	3.8774
6 (R = NO_2)	5.7918	5.8150	5.8889	5.9361

The highest obtained dipole moment for all compounds was observed in ethanol solvent. As can be seen in Table II, the dipole moment increases from the gas phase to a more polar solvent with the highest dipole moment occurring for compound **6** with a NO_2 substitute in ethanol solution with a value of ~5.94, while compound **1** has the lowest dipole moment in the gas phase (~1.91 D). It is noticeable that dipole moments are related to the influence of the nature of the substituents in the N_7 position. In this study, higher dipole moment values were observed in the compounds containing electron acceptors (*i.e.*, NO_2, Cl, CF_3) compared to those with electron-donor substituents (*i.e.*, H, CH_3, OH) in the studied solvents and gas phase. This is explained by the analysis of the charge values

* 1 D = 3.33564×10^{-30} C m

for the atoms of the six-membered ring. It is well known that the most negative charge is on the nitrogen N_7 atom in the considered compounds (Table III).

TABLE III. The calculated natural atomic charges (e) of the compounds **1**–**6**

Atom	Compound					
	1	**2**	**3**	**4**	**5**	**6**
C_4	0.17376	0.17432	0.17195	0.17411	0.16989	0.16800
C_5	–0.20438	–0.20499	–0.20450	–0.20493	–0.20340	–0.20311
N_7	–0.51340	–0.51206	–0.51398	–0.51070	–0.51524	–0.51537
C_8	0.33961	0.34003	0.33817	0.33997	0.33725	0.33565
S_9	0.30698	0.30570	0.31156	0.30587	0.31535	0.32064
N_{10}	–0.72158	–0.72200	–0.72168	–0.72398	–0.72088	–0.71983
C_{11}	0.15776	0.14786	0.15530	0.12327	0.17962	0.19328
H	0.35294	0.35237	0.35456	0.35246	0.35600	0.35771

Solvent effects

Solvent effects are important in stability phenomena because polarity differences between tautomers can induce important changes in their relative energies in solution.[27] The PCM calculations are used to evaluate the solvent effects on the 3-phenylbenzo[*d*]thiazole-2(3*H*)-imine derivatives. It is noted that the PCM model does not consider the existence of explicit solvent molecules; thus, specific solute–solvent interactions are not specified, and the studied solvation effects arise only from mutual solute-solvent electrostatic polarization. The lowest energy values of the considered compounds are obtained from aqueous solution calculations. The dipole moments are increased by increasing the solvent polarity and changing from gas to solution phases. Hence, increased stability with an electron-donating substituent in polar solvents could be associated with an increase of dipole moments (Table II). A plot of the dipole moment for the considered compounds versus dielectric constants is shown in Fig. 1.

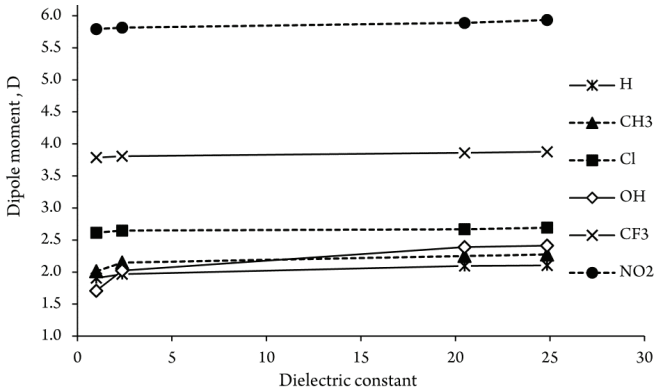

Fig. 1. Dielectric constant dependence of the dipole moments for the considered compounds.

The charge distributions of dipolar compounds are often altered considerably in the presence of the solvent field.[27] We have studied the charge distribution for compounds **1**–**6** in solvent and gas phases using the NBO technique. The charge distribution with increasing polarity varies for any atoms in solvents, *e.g.*, a regular increase of the negative charge was found for the N_7 atom derivatives when passing from the gas phase to a more polar solvent (Table II). The charge distribution of the charge on the N_7 atom is influenced by the nature of the substituent and the polarity of the solvents.

Natural population analysis (NPA) atomic charges

Natural population atomic charges calculation has an important role as the atomic charges cause the dipole moment, electronic structure, and molecular reactivity.[28] We have studied the charge distribution using NBO techniques in different media. The NPA analysis calculated using the NBO method at the M06-2x/6-311++G(d,p) theoretical level, and the achieved results are illustrated in details in the Supplementary material (Table S-I). In the case of benzene rings, all carbon atoms are assumed to be negative, but C_4 and C_{11} atoms are found to be positively charged, which may be due to the attachment of the N_7 atom to these carbon atoms in the five-membered ring. All hydrogen atoms in the studied molecules are found to be slightly positive as expected, so are other hydrogen atoms in the considered molecules.

It can be seen in Table III, the N_{10} atom has more negative charges while all the hydrogen atoms have positive charges. The result suggests that the atoms bonded to nitrogen atoms (H_{21} and C_{11}) are electron acceptors, and also indicates that the charge transfer from them (H_{21} and C_{11}) to the nitrogen atom. There is the order of the charge density at the hydrogen and N_{10} atom of the thiazole ring (NH), although the substituents are not directly attached to the thiazole ring. Therefore, differences in the strength of hydrogen bonding of the N–H group should be expected. The relationship between the C–H wavenumber shifts and calculated atomic charges of C_{16} (−0.1833 e) and N_{10} (−0.7216 e) also indicates that they take part in intramolecular hydrogen bonding. The influence of electronic effect resulting from the hyperconjugation and induction of the substituent (H, CH_3, Cl, OH, CF_3, NO_2) in the aromatic six-membered ring causes a large negatively charged value on the carbon atom C_{14}.

These calculations showed the electronegative nature of the O, S and N atoms. In compound **6**, the hydrogen atom H_{21} was the most electropositive atom among all of the hydrogen atoms (see Fig. S-1). The proton of the thiazole NH substituent possesses the highest value of 0.35771 e. In compounds **1**–**6**, the charges at this hydrogen site (H_{21} atom) were calculated to be 0.35294, 0.35237, 0.35456, 0.35246, 0.35600, and 0.35771 e, respectively. The order of the charge density at the NH hydrogen of the thiazole ring is: compound **6**>compound **5** >

compound **3** > compound **1** > compound **4** > compound **2**. This order agrees with the chemical sense where the electron-releasing substituent, namely the CH_3 substituent (compound **2**), decreases the positive charge at this H-site, while the NO_2 substituted derivative (compound **6**) has the highest positive NH proton, which agrees with its high electron-withdrawing character (–0.71983 e), although the substituent is not directly attached to the thiazole ring. It should be noted that the nitrogen atom corresponding to the NH group in the studied compounds has high negative values. The charge of this nitrogen atom (N10) is in the range of –0.71983 to –0.72398 e for the considered compounds. Instead, the charge on the nitrogen atom (N_3) of compounds **1**–**6** is calculated to be less (–0.51340, –0.51206, –0.51398, –0.51070, –0.51524 and –0.51537 e, respectively) negative than that on the NH one (N_{10} atom). Compound **6** showed a high positive value for the hydrogen atom (H_{21}) associated with the NO_2 substituent by 0.35771 e resulting from its bonding to the six-membered ring which is connected to the thiazole ring (Table S-I). Furthermore, all carbon atoms are negatively charged except for those attached to the strong electronegative N atom (C_4, C_8 and C_{11}). The charge at C_{14} atom in the six-membered ring for compounds **1**–**6** are calculated as –0.19844 (R=H), –0.02914 (R=CH_3), –0.04327 (R=Cl), 0.32693 (R=OH), –0.14892 (R=CF_3) and 0.06419 e (R=NO_2), respectively. The carbon atom of the C–Cl bond in compound **3** has a less negative charge of –0.04327 e than that for the C–CF_3 bond of compound **5** (–0.14892 e) that is in agreement with the higher electronegative nature of the chlorine atom (0.01100 e) compared to the carbon atom in the CF_3 substituent (1.08796 e). The phenolic oxygen atom of compound **4** has the highest negative value of –0.68134 e. As a result, the attached carbon atom, C_{14} (0.32693 e) in compound **4,** is found to have the most positive aromatic carbon atom (Table S-I).

Frontier molecular orbitals (FMO) analysis

Molecular orbitals and their properties, such as energy, are useful for physicists and chemists. This is also used in frontier electron density for predicting the most reactive position in π-electron systems and also explains several types of reaction in the conjugated system. Frontier molecular orbitals analysis is widely employed to explain the optical and electronic properties of organic compounds.[29] Knowledge of the highest occupied molecular orbitals (HOMO) and lowest unoccupied molecular orbitals (LUMO), and their properties namely their energy, is very useful to gauge the chemical reactivity of the molecules. During molecular interactions, the LUMO accepts the electrons and its energy corresponds to the electron affinity (EA), while the HOMO denotes electrons donors and its energy is associated with the ionization potential (IP).[30]

The HOMO–LUMO energy gap explains the concluding charge transfer interaction within the molecule and is useful in determining molecular electrical

transport properties. A molecule with a high frontier orbital gap (HOMO–LUMO energy gap) has low chemical reactivity and high kinetic stability, because it is energetically unfavorable to add an electron to the high-lying LUMO in order to remove electrons from the low-lying HOMO. For instance, the compounds that have a high HOMO–LUMO energy gap are stable, and hence are chemically harder than compounds having a small HOMO–LUMO energy gap.[31] Thus, it is clear from Table IV that compound **1** (R=H) is hard and more stable (less reactive), while compound **6** (R=NO_2) is soft and the least stable of all (more reactive) in the studied solvents and gas phases. The HOMO–LUMO gap decreases from compounds **1** to **6**. The minimum energy gap is achieved with an NO_2 substituent in the studied solvent and gas phases. Thus, this substituent increases the reactivity of the five-membered ring.

The global electrophilicity index (ω) is based on thermodynamic properties and measures the favorable change in energy when a chemical system attains saturation by addition of electrons. It can be defined as the decrease in energy due to flow of electrons from the donor (HOMO) to the acceptor (LUMO) in molecules. It also plays an important role in determining the chemical reactivity of system and is defined as $\omega = \mu^2/2\eta$, where η denotes the global chemical hardness ($\eta = (E_{LUMO}-E_{HOMO})/2$), and μ is the electronic chemical potential which describes the charge transfer ($\mu = (E_{LUMO}+E_{HOMO})/2$) within the system.[32–34]

Similarly, the electronegativity is a measure of attraction of an atom for electrons in the covalent bond, thus compound **6** has higher electronegativity, and it makes high charge flow occur. Also, the obtained results show that compound **6** (R=NO_2) is strong electrophilic while compound **2** (R=CH_3) is nucleophilic (see Table IV). Moreover, ΔN_{max} represents the maximum electronic charge ($\Delta N_{max} = -\mu/\eta$), S is the global softness ($S = 1/\eta$), and χ denotes the absolute electronegativity ($\chi = -\mu$) which is used to calculate the electron transfer direction. The absolute electronegativity is a good measure of the molecular ability to attract electrons to itself ($\chi = (IP+EA)/2$). It is noted that a small IP along with the high EA equal to a high nucleophilicity and a high electrophilicity, respectively. As can be seen in Table IV, compound **2** has the lowest IP and thus is the most nucleophilic species. All considered compounds in the solvents and gas phases have positive ΔN_{max} and act as an electron acceptor from their environment.

The global reactivity of compounds **1**–**6** is discussed in terms of the energy of the HOMO and LUMO, as well as the HOMO–LUMO energy gap, which was used for investigating kinetic stability and computed at the M06-2x/6 311++G(d,p) level (see Table IV). The large HOMO–LUMO energy gap shows that the compounds **1**–**6** are less kinetic stable against electronegativity. Thus, the kinetic stability of the studied compounds is as follows: **1** > **3** > **2** > **4** > **5** > **6**. The calculated results show that compounds **1** and **6** have the highest and lowest

kinetic stability in the solvent and gas phases, respectively. Similarly, the calculated ΔN_{max} values showed the same trend (Table IV). Moreover, because of the higher HOMO–LUMO energy gap, the global hardness increases for studied compounds as **1** > **3** > **2** > **4** > **5** > **6**, and the chemical reactivity decreases in the opposite order (**1** < **3** < **2** < **4** < **5** < **6**). The corresponding energy levels of the FMOs for studied compounds are shown in the Supplementary material (Fig. S--2). According to the investigation on the FMOs energy levels, we have found that the related electronic transfers happen between the HOMO and LUMO.

TABLE IV. Global reactivity descriptors calculated for 3-phenylbenzo[*d*]thiazole-2(3*H*)--imines (**1–6**)

Substituent	Parameter										
	E_{HOMO} eV	E_{LUMO} eV	ΔE eV	μ eV	η eV	ω eV	S eV^{-1}	χ eV	ΔN_{max}	IP eV	EA eV
Gas (ε = 1.00)											
H	–7.0096	–0.1510	6.859	–3.580	3.429	50.858	7.935	3.580	28.410	7.010	0.151
CH_3	–6.9487	–0.1524	6.796	–3.551	3.398	50.474	8.008	3.551	28.432	6.949	0.152
Cl	–7.1438	–0.3023	6.841	–3.723	3.421	55.131	7.955	3.723	29.616	7.144	0.302
OH	–6.9539	–0.2171	6.737	–3.586	3.368	51.928	8.079	3.586	28.966	6.954	0.217
CF_3	–7.2788	–0.6332	6.646	–3.956	3.323	64.081	9.634	3.956	32.397	7.279	0.633
NO_2	–7.4243	–1.7755	5.649	–4.600	2.824	101.929	8.189	4.600	44.318	7.424	1.776
Toluene (ε = 2.374)											
H	–7.0110	–0.1524	6.859	–3.582	3.429	50.897	7.935	3.582	28.420	7.011	0.152
CH_3	–6.9631	–0.1532	6.810	–3.558	3.405	50.589	7.992	3.558	28.436	6.963	0.153
Cl	–7.1465	–0.3061	6.840	–3.726	3.420	55.237	7.956	3.726	29.647	7.147	0.306
OH	–6.9816	–0.2386	6.743	–3.610	3.371	52.595	8.071	3.610	29.137	6.982	0.239
CF_3	–7.2769	–0.6558	6.621	–3.966	3.311	64.654	9.691	3.966	32.602	7.277	0.656
NO_2	–7.4213	–1.8057	5.616	–4.614	2.808	103.139	8.220	4.614	44.711	7.421	1.806
Acetone (ε = 20.493)											
H	–7.0134	–0.1488	6.865	–3.581	3.432	50.837	7.928	3.581	28.391	7.013	0.149
CH_3	–6.9639	–0.1589	6.805	–3.561	3.403	50.719	7.997	3.561	28.482	6.964	0.159
Cl	–7.1503	–0.3034	6.847	–3.727	3.423	55.200	7.948	3.727	29.623	7.150	0.303
OH	–6.9985	–0.2645	6.734	–3.631	3.367	53.290	8.082	3.631	29.349	6.998	0.264
CF_3	–7.2687	–0.6767	6.592	–3.973	3.296	65.150	9.755	3.973	32.798	7.269	0.677
NO_2	–7.4132	–1.8343	5.579	–4.624	2.789	104.278	8.256	4.624	45.105	7.413	1.834
Ethanol (ε = 24.852)											
H	–7.0134	–0.1494	6.864	–3.581	3.432	50.849	7.929	3.581	28.396	7.013	0.149
CH_3	–6.9637	–0.1586	6.805	–3.561	3.403	50.711	7.997	3.561	28.480	6.964	0.159
Cl	–7.1495	–0.3078	6.842	–3.729	3.421	55.294	7.955	3.729	29.659	7.150	0.308
OH	–6.9985	–0.2615	6.737	–3.630	3.368	53.223	8.078	3.630	29.324	6.998	0.262
CF_3	–7.2698	–0.6770	6.593	–3.973	3.296	65.164	9.783	3.973	32.800	7.270	0.677
NO_2	–7.4162	–1.8531	5.563	–4.635	2.782	105.067	8.255	4.635	45.340	7.416	1.853

NBO analysis

The NBO analysis has proved to be an effective tool for the chemical interpretation of hyperconjugative interaction and electron density transfer from the filled lone pair electron.[35] These changes in electron density are referred to as "delocalization" corrections to the zeroth-order natural Lewis structure to a stabilizing donor–acceptor interaction. In order to consider the different second-order perturbation energies (E_2) between the filled orbitals of one subsystem and vacant orbitals of another subsystem has been used, and it predicts the delocalization or hyperconjugation.[36] For each donor NBO(i) and acceptor NBO(j), the E_2 associated with the delocalization $i \rightarrow j$ is given by:[37]

$$E_2 = \Delta E_{ij} = q_i \left[F^2_{(i,j)} \Big/ (\varepsilon_i - \varepsilon_j) \right] \quad (1)$$

where q_i is the i^{th} donor orbital occupancy, ε_i and ε_j are diagonal elements (orbital energies), and $F_{(i,j)}$ is the off-diagonal NBO Fock matrix elements. The strong intramolecular hyperconjugative interactions of the σ and π electrons of C–C, C–H, N–H and C–N to the antibonding C–C, C–H, N–H and C–N bonds leads to stabilization of some part of the ring.

As can be seen from Table V, the $\sigma \rightarrow \sigma^*$ interactions have minimum delocalization energy compared to the $\pi \rightarrow \pi^*$ interactions.

TABLE V. The second-order perturbation energies E_2 for the most important charge transfer interactions in the compounds **1**–**6** in the gas phase

Donor NBO(i)	ED(i) a.u.	Acceptor NBO(j)	ED(j) a.u.	Interaction type	E_2 / kcal mol^{-1}					
					(**1**)	(**2**)	(**3**)	(**4**)	(**5**)	(**6**)
$\sigma_{N7–C8}$	1.97864	$\sigma^*_{C3–C4}$	0.02373	$\sigma_{N7–C8} \rightarrow \sigma^*_{C3–C4}$	3.12	3.13	3.11	3.13	3.08	3.07
		$\sigma^*_{C4–N7}$	0.03489	$\sigma_{N7–C8} \rightarrow \sigma^*_{C4–N7}$	2.62	2.61	2.61	2.61	2.60	2.57
		$\sigma^*_{N7–C11}$	0.04266	$\sigma_{N7–C8} \rightarrow \sigma^*_{N7–C11}$	2.52	2.52	2.52	2.53	2.51	2.50
		$\sigma^*_{C8–N10}$	0.00937	$\sigma_{N7–C8} \rightarrow \sigma^*_{C8–N10}$	1.65	1.66	1.62	1.65	1.60	1.56
		$\sigma^*_{N10–H21}$	0.00794	$\sigma_{N7–C8} \rightarrow \sigma^*_{N10–H21}$	2.64	2.64	2.66	2.63	2.67	2.69
		$\sigma^*_{C11–C12}$	0.02670	$\sigma_{N7–C8} \rightarrow \sigma^*_{C11–C12}$	1.03	1.01	1.04	0.96	1.11	1.19
		$\pi^*_{C11–C12}$	0.36802	$\sigma_{N7–C8} \rightarrow \pi^*_{C11–C12}$	0.89	0.90	0.93	0.98	0.92	0.93
$\sigma_{C8–N10}$	1.99183	$\sigma^*_{N7–C8}$	0.07155	$\sigma_{C8–N10} \rightarrow \sigma^*_{N7–C8}$	1.62	1.64	1.59	1.64	1.55	1.50
		$\sigma^*_{N10–H21}$	0.00794	$\sigma_{C8–N10} \rightarrow \sigma^*_{N10–H21}$	0.71	0.71	0.72	0.71	0.72	0.72
$\pi_{C8–N10}$	1.98974	$\pi^*_{C8–N10}$	0.30326	$\pi_{C8–N10} \rightarrow \pi^*_{C8–N10}$	1.77	1.77	1.76	1.78	1.74	1.71

$\sigma_{C4–C5}$	1.96633	$\sigma^*_{C3–C4}$	0.02373	$\sigma_{C4–C5} \rightarrow \sigma^*_{C3–C4}$	5.64	5.61	5.68	5.62	5.73	5.76
		$\sigma^*_{C3–H19}$	0.01307	$\sigma_{C4–C5} \rightarrow \sigma^*_{C3–H19}$	2.24	2.24	2.24	2.24	2.25	2.27

TABLE V. Continued

Donor NBO(*i*)	ED(*i*) a.u.	Acceptor NBO(*j*)	ED(*j*) a.u.	Interaction type	E_2 / kcal mol^{-1}					
					(**1**)	(**2**)	(**3**)	(**4**)	(**5**)	(**6**)
		$\sigma^*_{C4–N7}$	0.03489	$\sigma_{C4–C5} \rightarrow \sigma^*_{C4–N7}$	1.56	1.55	1.54	1.55	1.54	1.52
		$\sigma^*_{C5–C6}$	0.02103	$\sigma_{C4–C5} \rightarrow \sigma^*_{C5–C6}$	4.83	4.84	4.83	4.84	4.83	4.84
		$\sigma^*_{C6–H20}$	0.01400	$\sigma_{C4–C5} \rightarrow \sigma^*_{C6–H20}$	2.55	2.55	2.54	2.56	2.52	2.49
		$\sigma^*_{N7–C11}$	0.04266	$\sigma_{C4–C5} \rightarrow \sigma^*_{N7–C11}$	4.60	4.60	4.62	4.58	4.62	4.64
		$\sigma^*_{C8–S9}$	0.08416	$\sigma_{C4–C5} \rightarrow \sigma^*_{C8–S9}$	0.71	0.71	0.71	0.71	0.70	0.70
$\pi_{C4–C5}$	1.64246	$\pi^*_{C1–C6}$	0.35810	$\pi_{C4–C5} \rightarrow \pi^*_{C1–C6}$	30.29	30.39	–	30.41	–	–
		$\pi^*_{C2–C3}$	0.35677	$\pi_{C4–C5} \rightarrow \pi^*_{C2–C3}$	24.20	24.20	–	24.18	–	–
$LP(1)_{N7}$	1.67385	$\pi^*_{C2–C3}$	0.01442	$LP(1)_{N7} \rightarrow \pi^*_{C2–C3}$	0.51	0.51	< 0.5	0.51	< 0.5	< 0.5
		$\pi^*_{C4–C5}$	0.46854	$LP(1)_{N7} \rightarrow \pi^*_{C4–C5}$	44.53	44.73	45.22	44.72	44.40	43.63
		$\pi^*_{C8–N10}$	0.30326	$LP(1)_{N7} \rightarrow \pi^*_{C8–N10}$	60.07	60.39	59.25	60.42	58.29	57.08
		$\sigma^*_{C11–C12}$	0.02670	$LP(1)_{N7} \rightarrow \sigma^*_{C11–C12}$	4.89	4.97	5.00	5.00	4.73	4.52
		$\pi^*_{C11–C12}$	0.36802	$LP(1)_{N7} \rightarrow \pi^*_{C11–C12}$	8.34	7.99	8.90	6.88	11.06	13.12
		$\sigma^*_{C11–C16}$	0.02649	$LP(1)_{N7} \rightarrow \sigma^*_{C11–C16}$	4.89	4.89	4.85	5.26	4.53	4.34
$LP(1)_{S9}$	1.98211	$\sigma^*_{C4–C5}$	0.03264	$LP(1)_{S9} \rightarrow \sigma^*_{C4–C5}$	2.13	2.14	2.15	2.13	2.15	2.18
		$\sigma^*_{C5–C6}$	0.02103	$LP(1)_{S9} \rightarrow \sigma^*_{C5–C6}$	0.53	0.53	0.52	0.53	0.52	0.51
		$\sigma^*_{N7–C8}$	0.07155	$LP(1)_{S9} \rightarrow \sigma^*_{N7–C8}$	2.01	2.01	2.03	2.01	2.06	2.10
		$\sigma^*_{C8–N10}$	0.00937	$LP(1)_{S9} \rightarrow \sigma^*_{C8–N10}$	0.54	0.54	0.55	0.54	0.55	0.55
$LP(2)_{S9}$	1.77794	$\pi^*_{C4–C5}$	0.46854	$LP(2)_{S9} \rightarrow \pi^*_{C4–C5}$	19.95	19.99	23.29	19.94	23.23	23.28
		$\pi^*_{C8–N10}$	0.30326	$LP(2)_{S9} \rightarrow \pi^*_{C8–N10}$	30.82	30.77	31.19	30.81	31.46	31.79
$LP(1)_{N10}$	1.89453	$\sigma^*_{N7–C8}$	0.07155	$LP(1)_{N10} \rightarrow \sigma^*_{N7–C8}$	5.10	5.06	5.22	5.06	5.29	5.37

σ^*_{N7-C11}	0.04266	$LP(1)_{N10} \rightarrow \sigma^*_{N7-C11}$	0.69	0.69	0.68	0.68	0.66	0.63
σ^*_{C8-S9}	0.08416	$LP(1)_{N10} \rightarrow \sigma^*_{C8-S9}$	24.35	24.35	24.31	24.32	24.20	24.03

Therefore, the σ bonds have higher electron density than the π bonds. The strong intramolecular hyperconjugative interaction of the C_4–C_5 bond is formed by orbital overlap between the bonding orbital π_{C4-C5} to the corresponding antibonding orbital π^*_{C1-C6} with increasing electron density 0.3581 leading to the stabilization energy of 30.29 kcal mol^{-1}, which results in intramolecular charge transfer causing stabilization of the molecule. Similarly $\pi \rightarrow \pi^*$ interactions take place between the bonding π_{C4-C5} and antibonding orbitals π^*_{C2-C3} as well as the bonding π_{C8-N10} and antibonding orbitals $\pi^*_{C8-N10,}$ with an increase in electron density of 0.3568 and 0.30326, respectively, such that the respective bonds are stabilized by 24.20 (strong) and 1.77 kcal mol^{-1} (weak), respectively.

The NBO analysis also describes the bonding in terms of the natural hybrid orbital which emphasizes that the lone-pair of the nitrogen atom N_7 has an exclusive *p*-character (> 99.9%) and a low occupation number (1.67385 a.u.) in the studied compounds, leading to stronger stabilization interactions. Therefore, a very close to pure *p*-type lone-pair orbital participates in the electron donation to the π^*_{C4-C5} antibonding orbital for the $LP(1)_{N7} \rightarrow \pi^*_{C4-C5}$, and π^*_{C8-N10} antibonding orbital for the $LP(1)_{N7} \rightarrow \pi^*_{C8-N10}$ interactions (Table V). It is noted that the lone-pair $LP(1)N_{10}$ occupies a higher energy orbital (1.89453 a.u.) with *p*-character of ~34.4%. Also, the other lone-pair $LP(1)_{S9}$ has a high occupation number (1.98211 a.u.) with *p*-character (~63%). The lone-pair electrons are readily available for the interactions with the excited electrons of the acceptor antibonding orbital. The $LP(n) \rightarrow \pi^*$ interaction from the $LP(1)_{N7}$ donates an electron to the antibonding π^*_{C8-N10} and π^*_{C4-C5} orbitals with considerably higher stabilization energies of 60.07 and 44.53 kcal mol^{-1}, respectively. Similarly, intramolecular hyperconjugative interactions from the $LP(2)_{S9}$ to π^*_{C8-N10} and π^*_{C4-C5} leading to the stabilization energy of 30.82 and 19.95 kcal mol^{-1}, respectively. While the $LP(n) \rightarrow \sigma^*$ interaction takes place between the $LP(1)_{N10}$ to the σ^*_{C8-S9} antibonding orbital with the highest stabilization energy of 24.35 kcal mol^{-1} which results in intramolecular charge transfer causing stabilization of the molecular system.

As can be seen from Table V, the $\sigma \rightarrow \sigma^*$ interactions have minimum delocalization energy compared to the $\pi \rightarrow \pi^*$ interactions. Therefore, the σ bonds have higher electron density than the π bonds. The strong intramolecular hyperconjugative interaction of the C_4–C_5 bond is formed by orbital overlap between the bonding orbital π_{C4-C5} to the corresponding antibonding orbital π^*_{C1-C6} with increasing electron density 0.3581 leading to the stabilization energy of 30.29 kcal mol^{-1}, which results in intramolecular charge transfer causing stabilization

of the molecule. Similarly $\pi \rightarrow \pi^*$ interactions take place between the bonding π_{C4-C5} and antibonding orbitals π^*_{C2-C3} as well as the bonding π_{C8-N10} and antibonding orbitals $\pi^*_{C8-N10,}$ with an increase in electron density of 0.3568 and 0.30326, respectively, such that the respective bonds are stabilized by 24.20 (strong) and 1.77 kcal mol^{-1} (weak), respectively.

The NBO analysis also describes the bonding in terms of the natural hybrid orbital which emphasizes that the lone-pair of the nitrogen atom N_7 has an exclusive *p*-character (> 99.9%) and a low occupation number (1.67385 a.u.) in the studied compounds, leading to stronger stabilization interactions. Therefore, a very close to pure *p*-type lone-pair orbital participates in the electron donation to the π^*_{C4-C5} antibonding orbital for the $LP(1)_{N7} \rightarrow \pi^*_{C4-C5}$, and π^*_{C8-N10} antibonding orbital for the $LP(1)_{N7} \rightarrow \pi^*_{C8-N10}$ interactions (Table V). It is noted that the lone-pair $LP(1)N_{10}$ occupies a higher energy orbital (1.89453 a.u.) with *p*-character of ~34.4%. Also, the other lone-pair $LP(1)_{S9}$ has a high occupation number (1.98211 a.u.) with *p*-character (~63%). The lone-pair electrons are readily available for the interactions with the excited electrons of the antibonding acceptor orbital. The $LP(n) \rightarrow \pi^*$ interaction from the $LP(1)_{N7}$ donates an electron to the antibonding π^*_{C8-N10} and π^*_{C4-C5} orbitals with considerably higher stabilization energies of 60.07 and 44.53 kcal mol^{-1}, respectively. Similarly, intramolecular hyperconjugative interactions from the $LP(2)_{S9}$ to π^*_{C8-N10} and π^*_{C4-C5} leading to the stabilization energy of 30.82 and 19.95 kcal mol^{-1}, respectively. While the $LP(n) \rightarrow \sigma^*$ interaction takes place between the $LP(1)_{N10}$ to the σ^*_{C8-S9} antibonding orbital with the highest stabilization energy of 24.35 kcal mol^{-1} which results in intramolecular charge transfer causing stabilization of the molecular system.

Nucleus independent chemical shift (NICS) analysis

Aromaticity is a significant parameter associated with cyclic arrays of mobile electrons, and is a useful tool in organic chemistry. Theoretical criteria of aromaticity allow information on the physico-chemical properties of aromatic rings, namely structural chemical reactivity and stability. Schleyer *et al.* developed a simple and effective criterion for determining the aromaticity of different systems based on the diatropic current induced on placing the aromatic system in the external magnetic field. The NICS parameter was calculated as the negative shielding constant of a ghost atom (Bq) located at the ring center.[38] Negative NICS values indicate a diatropic ring current in the presence of an applied magnetic field (aromatic molecule) while the low negative or positive NICS value shows a paratropic ring current (non-aromatic or anti-aromatic molecule).[39,40] Here, the sets of points lying above and below, geometric center of rings were used at 2 Å. Their locations correspond with distances from −2 to 2 with 0.5 Å steps. The NICS(0) values calculated at the ring center that is influenced by σ

bonds, while the NICS(+2) and NICS(−2) values determined at the 2 Å above/ /below the plane (±2 Å) were more affected by the π-system. The maximum total diatropic current is observed at the 0.5 Å above/below the geometric of molecule in compounds **1**–**6**.

Interestingly, the *NICS* values at the minimum point of the six-membered rings are more negative (*i.e.*, specifying more aromaticity) than those of the five-membered rings for all the considered compounds (Fig. 2 and Table S-II of the Supplementary material). The *NICS* values of compound **2** in the studied solvent and gas phases calculated to be in ranges of –22.7965 to –23.2507 ppm, while the NICS values of compound **6** were slightly higher ranging from –24.4163 to –24.7124 ppm. For points located at the center of the six- and five-membered rings, and points located at ±2 Å ring centers (Table S-II) confirms that the aromaticity of compounds **1**–**6** changes with the varying dielectric constant of the media.

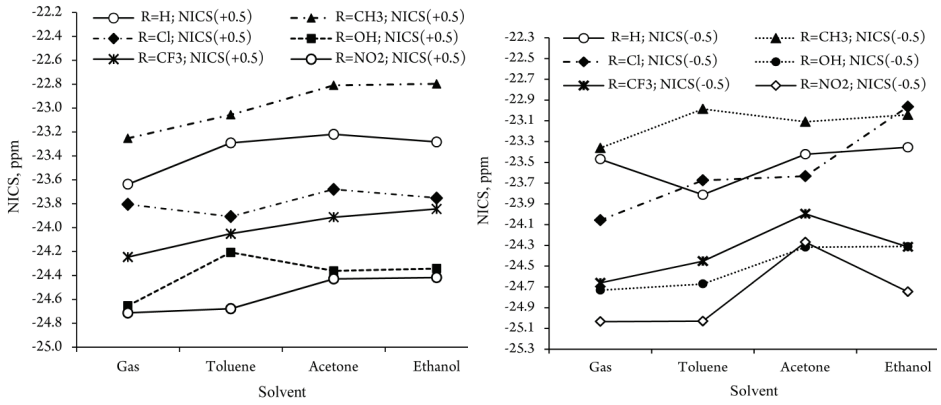

Fig. 2. Overall aromaticity of the studied compounds estimated as a function of *NICS versus* the considered solvents. *NICS* values at maximum diatropic current are tabulated (left: *NICS*(+0.5); right: *NICS*(−0.5)).

CONCLUSIONS

In this study, the solvation and substituent effects of the electron-releasing/withdrawing derivatives (*i.e.*, at the *para* position on the molecular structure of the synthesized compounds) **1**–**6** (R: H (**1**), CH_3 (**2**), Cl (**3**), OH (**4**), CF3 (**5**), NO_2 (**6**)) were investigated using the DFT/M06-2x/6-311++G(d,p) level of theory in selected solvents (toluene, acetone and ethanol) and in the gas phase by employing the polarizable continuum method model. In addition, the Fukui function, dipole moment, and distribution of electric charges on the atoms of the considered compounds were also studied with the same method and basis set. Frontier molecular orbital analysis showed that compound **6** in the selected solvents and gas phases has very low HOMO–LUMO energy gaps, and thus is kinetically less

stable. Chemical reactivity indices predict the highest activity for compound **6** in these media, whereas the lowest activity was decreased for compounds **4** and **1** in the gas phase and the studied solvents, respectively. The lowest HOMO–LUMO band gap is calculated for compound **6**, which results in it having interesting electronic properties. The calculated HOMO–LUMO energy gap corresponds to intramolecular hyperconjugative interactions $\pi \rightarrow \pi^*$. The results were confirmed by frontier molecular orbital (FMO) analysis, with energy gaps of 6.86, 6.80, 6.84, 6.74, 5.65 and 6.65 eV, respectively, and were determined for molecules **1–6**. The determined results show that the molecules **1** and **6** have the highest and lowest kinetic stability in the considered phases, respectively. NBO analysis showed intramolecular charge transfer causing stabilization of the molecule.

SUPPLEMENTARY MATERIAL

Additional data are available electronically at the pages of journal website: https://www.shd-pub.org.rs/index.php/JSCS/index, or from the corresponding author on request.

Acknowledgment. The authors would like to thank the referees for their valuable comments, which helped to improve the manuscript.

ИЗВОД

DFT СТУДИЈА И NBO АНАЛИЗА ЕФЕКАТА СОЛВАТАЦИЈЕ/СУПСТИТУЦИЈЕ КОД ДЕРИВАТА 3-ФЕНИЛБЕНЗО[*d*]ТИАЗОЛ-2(3*H*)-ИМИНА

MARZIEH MIAR[1], ABOLFAZL SHIROUDI[2], KHALIL POURSHAMSIAN[1], AHMAD REZA OLIAEY[1] и FARHAD HATAMJAFARI[1]

[1]*Chemistry Department, Tonekabon Branch, Islamic Azad University, Tonekabon, Iran;* [2]*Young Researchers and Elite Club, East Tehran Branch, Islamic Azad University, Tehran, Iran*

У овом раду, да би се утврдиле анализа природних орбитала веза (NBO), солватациони ефекти и ефекти супституената за електрон-отпуштајуће супституенте (CH_3, OH) и електрон-привлачеће деривате (Cl, NO_2, CF_3) у *para* положајима у молекулској структури синтетисаних деривата 3-фенилбензо[*d*]тиазол-2(3*H*)-имина **1–6**)H (**1**), CH_3 (**2**), Cl (**3**), OH (**4**), CF3 (**5**), NO_2 (**6**)=, у одабраним растварачима (ацетон, толуен и етанол) и у гасној фази, примењујући модел поларизабилног континуума (PCM), проучавани су на M06-2x/6-311++G(d,p) нивоу теорије. На релативну стабилност проучаваних једињења утиче могућност интрамолекулских интеракција између супституената и електрон донор/акцепторских центара тиазоловог прстена. Надаље, разматрана су атомска наелектрисања, хемијска термодинамика, енергетске особине, диполни моменти, и од језгра независни хемијски помаци (*NICS*), као и релативне стабилности ових једињења. Вредности диполних момената и HOMO–LUMO енергетски јаз откривају разне могућности за пренос наелектрисања унутар разматраних молекула. Анализа граничних молекулских орбитала (FMO) открива да једињење **6** има веома мали HOMO–LUMO енергетски јаз у разматраним фазама, па је тако мање стабилно. Добијени HOMO–LUMO енергетски јаз одговара унутармолекулској $\pi \rightarrow \pi^*$ хиперконјугационој интеракцији. Коначно, изведена је NBO анализа да се демонстрира пренос наелектрисања између локализованих веза и слободних електронских парова.

(Примљено 21. априла, ревидирано 10. августа, прихваћено 5. септембра 2020)

REFERENCES

1. M. Asif, *Int. J. Bioorg. Chem.* **2** (2017) 146 (https://doi.org/10.11648/j.ijbc.20170203.20)
2. M. Marzi, A. Shiroudi, K. Pourshamsian, A. R. Oliaey, F. Hatamjafari, *J. Sulfur Chem.* **40** (2019) 166 (https://doi.org/10.1080/17415993.2018.1548621)
3. M. Chhabra, S. Sinha, S. Banerjee, P. Paira, *Bioorg. Med. Chem. Lett.* **26** (2016) 213 (https://doi.org/10.1016/j.bmcl.2015.10.087)
4. J. Jiang, G. Li, F. Zhang, H. Xie, G. J. Deng, *Adv. Synth. Catal.* **360** (2018) 1622 (https://doi.org/10.1002/adsc.201701560)
5. M. G. Rabbani, T. Islamoglu, H. M. El-Kaderi, *J. Mater. Chem., A* **5** (2017) 258 (https://doi.org/10.1039/C6TA06342J)
6. R. K. Gill, R. K. Rawal, J. Bariwal, *Arch. Pharm.* **348** (2015) 155 (https://doi.org/10.1002/ardp.201400340)
7. P. C. Diao, W. Y. Lin, X. E. Jian, Y. H. Li, W. W. You, P. L. Zhao, *Eur. J. Med. Chem.* **179** (2019) 19 (10.1016/j.ejmech.2019.06.055)
8. M. A. Abdelgawad, R. B. Bakr, H. A. Omar, *Bioorg. Chem.* **74** (2017) 82 (https://doi.org/10.1016/j.bioorg.2017.07.007)
9. R. Ali, N. Siddiqui, *J. Chem.* (2013) 345198 (https://doi.org/10.1155/2013/345198)
10. D. Das, P. Sikdar, M. Bairagi, *Eur. J. Med. Chem.* **109** (2016) 89 (10.1016/j.ejmech.2015.12.022)
11. L. Shuai, J. Luterbacher, *ChemSusChem* **9** (2016) 133 (https://doi.org/10.1002/cssc.201501148)
12. L. Onsager, *J. Am. Chem. Soc.* **58** (1936) 1486 (https://doi.org/10.1021/ja01299a050)
13. L. Rivail, D. Rinaldi, *Theor. Chim. Acta* **32** (1973) 57 (https://doi.org/10.1007/BF01209416)
14. R. J. Hall, M. M. Davidson, N. A. Burton, I. H. Hillier, *J. Phys. Chem.* **99** (1995) 921 (https://doi.org/10.1021/j100003a014)
15. Z. Felegari, M. Monajjemi, *J. Theor. Comput. Chem.* **14** (2015) 1550021 (https://doi.org/10.1142/S0219633615500212)
16. Y. Zhao, D.G. Truhlar, *Theor. Chem. Acc.* **120** (2008) 215 (https://doi.org/10.1007/s00214-007-0310-x)
17. T. H. Dunning, Jr., *J. Chem. Phys.* **90** (1989) 1007 (https://doi.org/10.1063/1.456153)
18. S. Nigam, C. Majumder, S. K. Kulshreshtha, *J. Chem. Sci.* **118** (2006) 575 (https://doi.org/10.1007/BF02703955)
19. P. v. R. Schleyer, M. Manoharan, Z. X. Wang, B. Kiran, H. J. Jiao, R. Puchta, N. Hommes, *Org. Lett.* **3** (2001) 2465 (https://doi.org/10.1021/ol016217v)
20. P. v. R. Schleyer, H. Jiao, B. Goldfuss, P. K. Freeman, *Angew. Chem. Int. Ed. Engl.* **34** (1995) 337 (https://doi.org/10.1002/anie.199503371)
21. P. v. R. Schleyer, C. Maerker, A. Dransfeld, H. Jiao, N. J. R. V. E. Hommes, *J. Am. Chem. Soc.* **118** (1996) 6317 (https://doi.org/10.1021/ja960582d)
22. A. E. Reed, R. B. Weinstock, F. Weinhold, *J. Chem. Phys.* **83** (1985) 735 (https://doi.org/10.1063/1.449486)
23. J. K. Badenhoop, F. Weinhold, *Int. J. Quantum. Chem.* **72** (1999) 269 (https://doi.org/10.1002/(SICI)1097-461X(1999)72:4<269::AID-QUA9>3.0.CO;2-8)
24. *Gaussian 09, Revision C.01*, Gaussian, Inc., Wallingford, CT, 2009
25. *GaussView5.0.9*, Gaussian, Inc., Wallingford, CT
26. E. D. Glendening, J. K. Badenhoop, A. E. Reed, J. E. Carpenter, J. A. Bohmann, C. M. Morales, F. Weinhold, *NBO 5.0.,* Theoretical Chemistry Institute, University of Wisconsin, Madison, WI, 2001

27. I. M. Alecu, J. Zheng, Y. Zhao, D. G. Truhlar, *J. Chem. Theory Comput.* **6** (2010) 2872 (https://doi.org/10.1021/ct100326h)
28. K. Fukui, T. Yonezawa, H. Shingu, *J. Chem. Phys.* **20** (1952) 722 (https://doi.org/10.1063/1.1700523)
29. L. Padmaja, C. Ravi Kumar, D. Sajan, I. H. Joe, V. S. Jayakumar, G. R. Pettit, *J. Raman Spectrosc.* **40** (2009) 419 (https://doi.org/10.1002/jrs.2145)
30. J. Aihara, *J. Phys. Chem., A* **103** (1999) 7487 (https://doi.org/10.1021/jp990092i)
31. Y. Ruiz-Morales, *J. Phys. Chem., A* **106** (2002) 11283 (https://doi.org/10.1021/jp021152e)
32. R. G. Parr, L. Szentpaly, S. Liu, *J. Am. Chem. Soc.* **121** (1999) 1922 (https://doi.org/10.1021/ja983494x)
33. R. G. Parr, R. G. Pearson, *J. Am. Chem. Soc.* **105** (1983) 7512 (https://doi.org/10.1021/ja00364a005)
34. R. G. Parr, R. A. Donnelly, M. Levy, W. E. Palke, *J. Chem. Phys.* **68** (1978) 3801 (https://doi.org/10.1063/1.436185)
35. Y. Yang, W. Zhang, X. Gao, *Int. J. Quantum Chem.* **106** (2006) 1199 (https://doi.org/10.1002/qua.20873)
36. J. E. Carpenter, F. Weinhold, *J. Mol. Struct., Theochem* **169** (1988) 41 (https://doi.org/10.1016/0166-1280(88)80248-3)
37. A. R. Oliaey, A. Shiroudi, E. Zahedi, M. S. Deleuze, *React. Kin. Mech. Catal.* **124** (2018) 27 (https://doi.org/10.1007/s11144-017-1332-6)
38. P. v. R. Schleyer, H. Jiao, *Pure Appl. Chem.* **68** (1996) 209 (http://dx.doi.org/10.1351/pac199668020209)
39. T. M. Krygowski, M. Cyranski, A. Ciesielski, B. Swirska, P. Leszczynski, *J. Chem. Inf. Comput. Sci.* **36** (1996) 1135 (https://doi.org/10.1021/ci960367g)
40. S. Badoglu, S. Yurdakul, *Struct. Chem.* **21** (2010) 1103 (https://doi.org/10.1007/s11224-010-9651-5).